

Cooperative Distributed Energy Scheduling for Smart Homes Applying Stochastic Model Predictive Control

Mehdi Rahmani-andebili¹ and Haiying Shen²

¹ Department of Electrical and Computer Engineering, Clemson University, Clemson, SC 29631, USA

² Department of Computer Science, University of Virginia, Charlottesville, VA 22904, USA
mehdir@g.clemson.edu, hs6ms@virginia.edu

Abstract- In this study, distributed energy resources scheduling problem of the set of smart homes (SHs) is investigated considering their cooperation with their neighbors and applying a stochastic model predictive control (MPC). Herein, every SH has a variety of sources and each SH is able to transact power with the local distribution company (DISCO) through the grid and with other connected SHs. The challenges of problem include modeling the technical and economic constraints of sources and dealing with the variability and uncertainties concerned with the power of photovoltaic (PV) panels that make the problem a mixed-integer nonlinear programming (MINLP), dynamic, and stochastic optimization problem. In order to handle the variability and uncertainties of problem, a stochastic MPC is applied. The numerical study demonstrates that cooperation of SHs in the energy scheduling problem has a high potential for minimizing operation cost of SHs.

Index Terms- Cooperative distributed energy scheduling, smart home (SH), and stochastic model predictive control (MPC).

I. INTRODUCTION

To mitigate the energy security and environmental issues caused by burning fossil fuels in the thermal power plants, installing renewables as the cost-effective and carbon-free source of energy is proposed [1]. Building sector has a huge potential for decreasing cost of energy use, increasing energy efficiency, and decreasing the carbon footprint by including renewables [2]. The U.S. Energy Information Administration (EIA) estimates that 37% of end use electricity in the U.S. is consumed in the residences [3]. In addition, the buildings are responsible for 36% of the carbon emissions in the U.S. [3-4].

Advances in the technology are able to change a home into a smart home (SH) that allows the occupant to control the energy consumption of the home [5-6]. SHs are equipped with devices and sources that coordinate with one another to achieve a common set of goals that benefit the occupants [7]. They are able to connect to each other, share their energy sources, and exchange electricity. In other words, each SH can provide energy to other SHs and purchase energy from other SHs. Also, every SH can deliver its extra energy to the grid and sell it to the local distribution company (DISCO), but at a lower price compared to the purchasing price [8].

In this study, a cooperative distributed energy scheduling approach is applied to solve this problem for the set of the SHs. In this method, every SH takes into account its available energy resources such as DG, PV panels, and battery of plug-in electric vehicle (PEV), collects the information of the available energy of the connected SHs and their proposed prices, and conducts the energy scheduling in a cooperative distributed way. However, there are several challenges in solving the problem listed below.

- PV panels as the intermittent source of energy have the feature of uncertainty in their power that makes the energy scheduling problem a stochastic optimization problem.
- In addition, the power of PV panels has a large degree of variability that change the energy scheduling problem into a dynamic (time-varying) optimization problem.
- There are several economic and technical constraints for the DG and the battery of the PEV that make the problem a mixed integer nonlinear programming (MINLP) problem.

The studies presented in [9-13] have investigated energy scheduling problem for the set of SHs. However, in [9-11] and [13], the problem is not a cooperative distributed energy scheduling problem, since the cooperation of the SHs have been disregarded and the problem has been solved by a centralized approach. However, the centralized optimization techniques have the so-called curse of dimensionality when the problem is large and complex [14]. In other words, the computational complexity and computation latency of the problem grow exponentially when the size of the problem is increased. Therefore, the centralized optimization is not applicable when the problem has a large number of variables or the state of the problem is changed dynamically. In addition, the privacy of the SHs might be jeopardized in a centralized optimization approach because all the economic and technical information of the SHs must be available for the control center [15].

In [9] and [11-12], the presence of different energy resources have not been modeled in the problem. In other words, renewable energy resources have been disregarded in [9] and [11-12], energy storage has not been modeled in [9] and [12], and presence of DG has not been taken into consideration in [9]. Also, the defined energy scheduling problem does not have any dynamic and adaptive characteristics in [10-11]. In other words, the problem has been optimized once for the whole operation period (one day), while the optimization of the problem must be updated at every time step (e.g., every hour, every five minutes, or ...) due to the time-varying feature of the power of renewables or load demand. In this study, the aforementioned challenges are addressed by applying the proposed techniques presented in Section II. In Section III, the problem is formulated. The numerical studies are done in Section IV, and Section V concludes the paper.

II. PROPOSED TECHNIQUE

A. Cooperative Distributed Energy Scheduling

Fig. 1 illustrates the concept of the cooperative distributed optimization for a system with five SHs. As can be seen, each SH electrically connects to a number of other SHs for energy transaction. In other words, every SH can provide energy to its

connected SHs and also purchase energy from them. Herein, it is assumed that every SH can exchange the information just with its connected SHs. The information includes the value of available energy and price for transacting power between two SHs.

Based on the concept of the introduced approach for the cooperative distributed energy scheduling, at every time step, in parallel to other SHs, every SH randomly selects its counterpart (one of the connected SHs), and solves its own energy scheduling problem considering the received information from the selected cooperator. Then, every SH randomly changes its cooperator and share the updated information with one another. This process is repeated several times until no significant improvement is observed in the value of the objective function of each SH.

B. Stochastic Model Predictive Control (MPC)

1) Stochastic approach

The stochastic approach includes forecasting the solar irradiances and modeling the uncertainty of the predictions by defining some effective scenarios.

a) Forecasting the value of the uncertain states

The uncertain states of the problem include the values of solar irradiances (ρ) over the optimization time horizon which are predicted using the neural network available in MATLAB. The historical values of the solar irradiances are entered into the neural network to predict the values of the solar irradiances over the optimization time horizon. The historical data of the solar irradiances are the real solar irradiances recorded in Clemson, SC 29634, USA in July 2014. About 70% of the data is used for training the neural network and 30% of the data is used for validation and testing. The set of the predicted solar irradiances ($\tilde{\rho}$) can be presented as (1). As can be seen, the duration of forecasting time horizon is 12 time steps (n_τ is equal to 12).

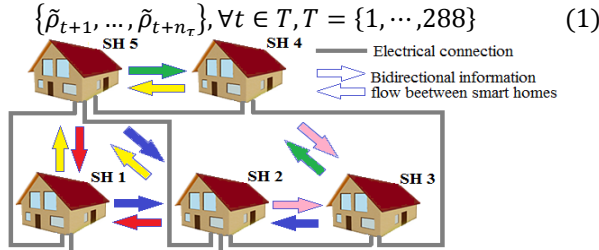


Fig. 1. Applying cooperative distributed optimization on a system with five SHs.

b) Modeling uncertainties of the forecasted data

Fig. 2 (a) illustrates the predicted and measured solar irradiances for the current time step (t) and past time steps ($1, 2, \dots, t-1$), and also the predicted solar irradiances for every time step of the optimization time horizon ($t+1, \dots, t+n_\tau$). As can be seen, the previously forecasted solar irradiances ($\tilde{\rho}$) are compared with the real solar irradiances (measured data) and the value of error of the predictions are calculated. Then, as can be seen in Fig. 2 (b), redundancy of the prediction errors respect to the value of the prediction errors are plotted on a chart. After that, an appropriate probability density function is found for the prediction errors, as can be seen in Fig. 2 (c). It is observed that the prediction errors can be nearly fitted on a Normal probability density function with an appropriate standard deviation (σ^{Er}). Finally, the curve is

divided into four areas to define four distinct values for the prediction inaccuracy with occurrence probabilities about 15.87%, 34.13%, 34.13%, and 15.87% related to $-2\sigma^{Er}$, $-\sigma^{Er}$, σ^{Er} , and $2\sigma^{Er}$, respectively. The value of σ^{Er} is updated in the next predictions in the optimization procedure of the problem ($1, 2, \dots, t, \dots, 288$).

Herein, four scenarios ($s \in S, S = \{1, \dots, n_s\}$, where n_s is 4) for solar irradiance corresponding to $\rho_{h,t,s} \in \{\tilde{\rho}_{h,t} - 2\sigma^{Er}, \tilde{\rho}_{h,t} - \sigma^{Er}, \tilde{\rho}_{h,t} + \sigma^{Er}, \tilde{\rho}_{h,t} + 2\sigma^{Er}\}$ with occurrence probabilities (Ω^{PV}) 15.87%, 34.13%, 34.13%, and 15.87%, respectively, are considered. In other words, at every time step, the problem is solved four times and every time, one of the above mentioned values are considered for the value of the solar irradiance.

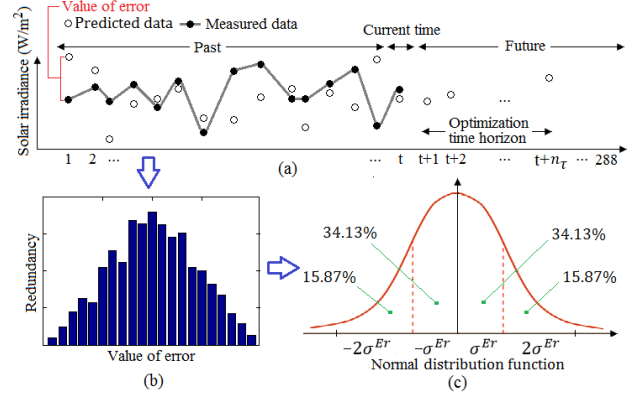


Fig. 2. Modeling uncertainties of the forecasted data.

2) Model Predictive Control

MPC as a well-established technique in control engineering is capable of controlling a multi-variable constrained system by taking the control actions from the solution of an online optimization problem and repetitively predicting the system behavior [16]. The concept of the single-time scale MPC is illustrated in Fig. 3 [17]. As can be seen, at every time step (t), the optimization time horizon ($t+1, \dots, t+n_\tau$) is updated, and then the value of the forward-looking objective function (F_t^{FL}) is minimized; however, just the variables of the next time step ($t+1$) are accepted as the decision variables. The forward-looking objective function is sum of the values of the time step objective functions (F_t) over the optimization time horizon, as can be seen in (2). Next, the current time step is $t+1$ and the updated optimization time horizon is $t+2, \dots, t+n_\tau+1$. Now, the value of the updated forward-looking objective function (F_{t+1}^{FL}) is minimized and the variables of the next time step ($t+2$) are accepted as the decision variables. This procedure that demonstrates the dynamic and adaptability characteristics of MPC is repeated for every time step of the operation period (one day).

$$F_t^{FL} = \sum_{\tau=1}^{n_\tau} F_{t+\tau} \quad (2)$$

C. Optimization Tool

The energy scheduling problem of the SH is a MINLP problem. In this study, GA-LP technique as the combination of genetic algorithm (GA) and Linear Programming (LP) is applied to solve the energy scheduling problem of the SH. Other optimization algorithms could be used instead of GA; however, the capability of GA for parallel optimization and its

competence in complex and nonlinear environments are the main reasons for the utilization of GA [18].

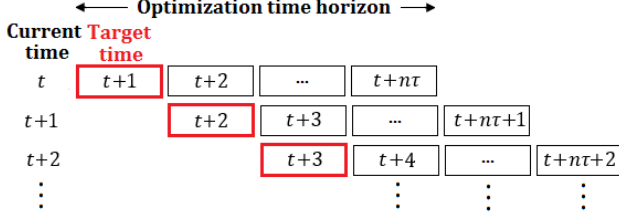


Fig. 3. The concept of the single-time scale model predictive control [17].

Herein, the GA is applied to address the nonlinearity of the problem and the LP is applied to quickly find the globally optimal solution. Moreover, the GA and LP techniques deal with the discrete variables (x^{DG}, x^{PEV}) and the continuous variables ($P^{DG}, P^{PEV}, P^{Grid}$) of the problem, respectively.

The discrete variables of the problem handled by the GA include the status of the DG (x^{DG}) and the status of the battery of the PEV (x^{PEV}) in every time step of the optimization time horizon, as can be seen in (3). Herein, the values of “0” and “1” for the x^{DG} mean “off” and “on”, respectively. Also, the values of “-1”, “0”, and “1” for the x^{PEV} mean charging, idle, and discharging, respectively.

$$\left\{ \begin{array}{ccc} x_t^{DG} & \dots & x_{t+n\tau}^{DG} \\ x_t^{PEV} & \dots & x_{t+n\tau}^{PEV} \end{array} \right\}, \forall t \in T \quad (3)$$

Based on this, the dimensions of the defined chromosome in the applied GA are $n_\tau \times 3$, as can be seen in Fig. 4. Herein, one bit (gene) for indicating status of the DG (“0” for “off” and “1” for “on”) and two bits for indicating the status of the battery of the PEV (“00” and “10” for idle, “01” for discharging, and “11” for charging) are considered.

	DG		PEV	
t+1	0/1	0/1	0/1	0/1
t+2	0/1	0/1	0/1	0/1
⋮	⋮	⋮	⋮	⋮
t+n τ	0/1	0/1	0/1	0/1

Fig. 4. The structure of the defined chromosome in the applied GA.

In addition, the continuous variables of the problem optimized by the LP include the value of power of the DG (P^{DG}), the value of generated or consumed power of the battery of the PEV (P^{PEV}), the value of transacted power with the DISCO through the electricity grid (P^{Grid}), and the value of transacted powers with the connected SHs ($P_{h,t,h'}^N, \forall h \in H'$) in every time step of the optimization time horizon, as can be seen in (4).

$$\left\{ \begin{array}{ccc} P_{h,t}^{DG} & \dots & P_{h,t+n\tau}^{DG} \\ P_{h,t}^{PEV} & \dots & P_{h,t+n\tau}^{PEV} \\ P_{h,t}^{Grid} & \dots & P_{h,t+n\tau}^{Grid} \\ P_{h,t,1}^N & \dots & P_{h,t+n\tau,1}^N \\ \vdots & \dots & \vdots \\ P_{h,t,n_{h'}}^N & \dots & P_{h,t+n\tau,n_{h'}}^N \end{array} \right\}, \forall h \in H, H' = \{1, \dots, n_{h'}\}, \forall t \in T \quad (4)$$

III. PROBLEM FORMULATION

A. Objective Function

The goal of every SH is minimizing the value of the stochastic forward-looking objective function over the

optimization time horizon (\mathbb{F}^{FL}) subject to the constraints. As can be seen in (5), the value of the stochastic forward-looking objective function is determined by summing the values of the forward-looking objective functions (F^{FL}) weighted by the corresponding occurrence probability (Ω^{PV}). In other words, the value of the stochastic forward-looking objective function is equal to the expected value of the forward-looking objective function. The forward-looking objective function ($F_{h,t,s}^{FL} = \sum_{\tau=1}^{n\tau} F_{h,t+\tau,s}$) has been presented in (2). The time step objective function (F) that includes different cost and income terms is presented in (6). These terms include fuel cost of the DG ($C^{F,DG}$), carbon emissions cost of the DG ($C^{E,DG}$), start up cost of the DG ($C^{STU,DG}$), shut down cost of the DG ($C^{SHD,DG}$), switching cost of the battery of the PEV ($C^{SW,PEV}$), cost or benefit due to power transactions with the grid ($P^{Grid} \times \hat{\pi}^{DISCO}$), and cost or benefit because of power transactions with the connected SHs ($\sum P^N \times \pi^N$).

$$\min \mathbb{F}_{h,t}^{FL} = \min \sum_{s \in S} F_{h,t,s}^{FL} \times \Omega_s^{PV}, \forall h \in H, \forall t \in T \quad (5)$$

$$F_{h,t,s} = \left\{ \begin{array}{l} [C_{h,t}^{F,DG}] + [C_{h,t}^{E,DG}] \\ + [(1 - x_{h,t-1}^{DG}) \times x_{h,t}^{DG} \times C_h^{STU,DG}] \\ + [x_{h,t-1}^{DG} \times (1 - x_{h,t}^{DG}) \times C_h^{SHD,DG}] + \\ [x_{h,t}^{PEV} \times C_h^{SW,PEV}] + [P_{h,t}^{Grid} \times \hat{\pi}_t^{DISCO}] \\ + \left[\sum_{h' \in H'} P_{h,t,h'}^N \times \pi_{h,t,h'}^N \right] \end{array} \right\}, \forall h \in H, \forall t \in T \quad (6)$$

The switching of the battery of PEV (\hat{x}^{PEV}) is determined using (7). If the status of the battery in the current time step (x_t^{PEV}) is the same as the previous time step (x_{t-1}^{PEV}), the switching indicator is zero; otherwise, it is one.

$$\hat{x}_{h,t}^{PEV} = \begin{cases} 0 & x_{h,t-1}^{PEV} = x_{h,t}^{PEV} \\ 1 & x_{h,t-1}^{PEV} \neq x_{h,t}^{PEV} \end{cases}, \forall h \in H, \forall t \in T \quad (7)$$

In (8), φ is the coefficient applied by the local DISCO to determine the price of selling power to the DISCO by a SH based on the net energy metering (NEM) plan [8]. In the NEM plan, every SH can deliver its extra power to the grid and sell it to the local DISCO at a lower price compared to the purchasing price from the local DISCO [8]. Herein, $P^{Grid} > 0$ means the SH purchases power from the local DISCO and $P^{Grid} < 0$ means the SH sells power to the local DISCO.

$$\hat{\pi}_t^{DISCO} = \begin{cases} \pi_t^{DISCO} & P_t^{Grid} > 0 \\ \varphi \times \pi_t^{DISCO} & P_t^{Grid} < 0 \end{cases}, \forall h \in H, \forall t \in T \quad (8)$$

The price of the transacted energy between two SHs is assessed based on the marginal cost of the installed DG in the power exporter SH; however, if there is no DG in the power exporter SH, the price is determined based on the marginal cost of the installed DG in the power importer SH. Moreover, if every SH has a DG, the price of electricity transaction is determined based on the average value of the generation costs of the DGs. The marginal cost of a DG can be determined using (9) [19].

$$\pi_{h,t}^N = \frac{\partial (C_{h,t}^{F,DG} + C_{h,t}^{E,DG})}{\partial P_{h,t}^{DG}}, \forall h \in H, \forall t \in T \quad (9)$$

The fuel cost function and carbon emissions function of every DG are quadratic polynomials presented in (10) and (11), respectively [19]. Herein, are the set of z_1^F, z_2^F, z_3^F and z_1^E, z_2^E, z_3^E are the fuel cost coefficients and carbon emissions

coefficients of the DG, respectively. Also, β^E is the value of penalty for carbon emissions.

$$C_{h,t}^{FDG} = x_{h,t}^{DG} \times \left(z_{1,h}^F \times (P_{h,t}^G)^2 + z_{2,h}^F \times (P_{h,t}^G) + z_{3,h}^F \right) \quad \forall h \in H, \forall t \in T \quad (10)$$

$$C_{h,t}^{EDG} = x_{h,t}^{DG} \times \beta^E \times \left(z_{1,h}^E \times (P_{h,t}^G)^2 + z_{2,h}^E \times (P_{h,t}^G) + z_{3,h}^E \right), \quad \forall h \in H, \forall t \in T \quad (11)$$

The value of the switching cost of the battery of a PEV is determined based on the value of total cumulative ampere-hours throughput of the battery (ξ^{PEV}) in its life cycle and the value of the initial price of the battery (Pr^{PEV}). In fact, considering this cost term prevents the battery of the PEV from unnecessary switching that is harmful to its life span.

$$C_h^{SWPEV} = \frac{Pr_h^{PEV}}{\xi_h^{PEV}}, \forall h \in H \quad (12)$$

B. Constraints

1) Supply-demand balance

The sum of power of DG, power of PV panels, power of battery of PEV, the transacted power with the connected SHs, and the transacted power with the DISCO through the grid must be equal to the load demand (D^L) in every SH and at every time step of the operation period. Herein, the transacted power with the connected SHs is considered positive if the SH imports power and it is negative if the SH exports power.

$$\left(x_{h,t}^{DG} \times P_{h,t}^{DG} \right) + \left(x_{h,t}^{PEV} \times P_{h,t}^{PEV} \right) + P_{h,t,s}^{PV} + P_{h,t}^{Grid} + \sum_{h' \in H'} P_{h,t,h'}^N = D_{h,t}^L, \forall h \in H, \forall t \in T, \forall s \in S \quad (13)$$

2) Power limits of the diesel generator

The maximum power limit ($\overline{P^{DG}}$) and minimum power limit ($\underline{P^{DG}}$) of every DG is presented in (14).

$$x_{h,t}^{DG} \times \left(\underline{P_h^{DG}} \leq P_{h,t}^{DG} \leq \overline{P_h^{DG}} \right), \forall h \in H, \forall t \in T \quad (14)$$

3) Minimum up/down time limits of the diesel generator

The duration that the DG is continuously “on” (Δt^{DG_ON}) and “off” (Δt^{DG_OFF}) must be more than the rated minimum up time (MUT^{DG}) and minimum down time (MDT^{DG}).

$$\Delta t_h^{DG_ON} \geq MUT_h^{DG}, \forall h \in H, \forall t \in T \quad (15)$$

$$\Delta t_h^{DG_OFF} \geq MDT_h^{DG}, \forall h \in H, \forall t \in T \quad (16)$$

4) Power limits of the battery of the PEV

The battery of the PEV can act as a load or generator by being charged or discharged, respectively; however, the power of battery of PEV must be in the rated range. Herein, $\overline{P^{PEV}}$ is the rated power of battery of PEV.

$$x_{h,t}^{PEV} \times \left(-\overline{P_h^{PEV}} \leq P_{h,t}^{PEV} \leq \overline{P_h^{PEV}} \right), \forall h \in H, \forall t \in T \quad (17)$$

5) Depth of discharge limit of the battery of the PEV

In order to prolong the life time of the battery of PEV, the battery must not be discharged more than the allowable DOD. Moreover, the battery has a definite capacity that cannot be charged more than that.

$$DOD_h^{PEV} \leq SOC_{h,t}^{PEV} \leq 100, \forall h \in H, \forall t \in T \quad (18)$$

6) Disconnection of the PEV from the SH

This constraint indicates that the PEV is being used by its driver and the PEV is no longer connected to the SH in this interval ($\Delta t_{Dep-Arr}$), as can be seen in (19).

$$x_{h,t}^{PEV} = 0, \forall h \in H, t \in \{ \Delta t_{Dep-Arr} \} \quad (19)$$

7) Full charge constraint for battery of PEV before departure

By holding this constraint, the owner of the PEV is confident that the PEV will have full charge at the desirable time (t_{Dep}) and ready to be used.

$$SOC_{h,t_{Dep}}^{PEV} = 100, \forall h \in H \quad (20)$$

8) Maximum accessible power from a connected SH

The power that the SH can import from a connected SH (P^N) must be less than the available power of connected SH (P^A) at every time step of the optimization period.

$$P_{h,t,h'}^N \leq P_{h',t}^A, \forall h \in H, \forall h' \in H', \forall t \in T \quad (21)$$

where,

$$P_{h',t}^A = \begin{cases} x_{h',t}^{DG} \times \left(\overline{P_{h',t}^{DG}} - P_{h',t}^{DG} \right) + \overline{P_{h',t}^{PEV}} - P_{h',t}^{PEV} & x_{h',t}^{PEV} = 1 \\ x_{h',t}^{DG} \times \left(P_{h',t}^{DG} - \overline{P_{h',t}^{DG}} \right) & x_{h',t}^{PEV} \neq 1 \end{cases} \quad (22)$$

Based on (22), if the battery of the PEV of a connected SH is in discharging status ($x_{h',t}^{PEV} = 1$), the battery has available capacity about $(\overline{P_{h',t}^{PEV}} - P_{h',t}^{PEV})$ to help the SH. Also, if the DG of a connected SH is in “on” status, the DG has available capacity about $(\overline{P_{h',t}^{DG}} - P_{h',t}^{DG})$ to help the SH.

IV. NUMERICAL STUDY

All the simulations are done in MATLAB environment using the Intel Xeon Sever with 64 GB RAM. Fig. 5 illustrates the configuration of the case study that include five SHs with different set of sources including PV panels installed on the roof of the SH, PEV, DG, and electrical distribution grid. In addition, every SH has connections to some of the other SHs. The technical data for different types of the DGs are presented in TABLE I. Furthermore, the value of other parameters of system and problem are presented in TABLE II. Fig. 6 shows the electricity price proposed by the local DISCO in every time step (five minutes) of the operation period (one day).

The load demand patterns of SHs 1-5 are shown in Figs. 7, 9, 11, 13, and 15, respectively. Moreover, SH 4 and SH 5 have PEV of type 1 and type 2, respectively. In addition, the power patterns of the PV panels related to SHs 2-5 are illustrated in Figs. 9, 11, 13, and 15, respectively.

A. Without energy scheduling and non-cooperative energy scheduling

TABLE III presents the operation cost of every individual SH and the set of SHs without energy scheduling of SHs (scenario 1) and with non-cooperative energy scheduling (scenario 2). For the first scenario, the power of PV panels are considered as the negative demand and then it is added to the load demand of every individual SH. In addition, at every time step, the extra power of every SH is directly delivered to the grid and sold to the local DISCO. As can be seen, the total operation cost of the set of SHs for the first and second scenario are about \$66.01/day and \$43.59/day, respectively.

B. Cooperative distributed energy scheduling

The daily operation cost of the set of SHs and every individual SH, and also the optimal schedule of energy resources of SHs in the cooperative distributed energy scheduling (scenario 3) are presented in TABLE III and Figs. 7-16, respectively. As can be seen, the operation cost of every SH is reduced and SH 1 not only removes its operation cost, but also it makes income. Moreover, the total operation cost of the set of SHs is decreased to about \$30.82/day.

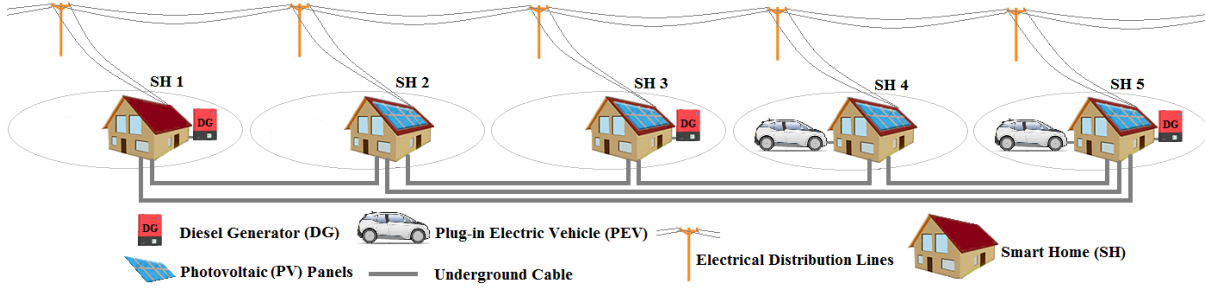


Fig. 5. The configuration of the system under study.

TABLE I

TECHNICAL DATA OF DIFFERENT TYPES OF THE DGs.

Parameter	Type 1	Type 2	Type 3
z_1^F (¢/kWh ²)	0.00324	0.00243	0.00491
z_2^F (¢/kWh)	3.96	9.94	7.85
z_3^F (¢)	0	0	0
z_1^E (kg/kWh ²)	0.0007	0.0008	0.0008
z_2^E (kg/kWh)	0.39	0.94	0.61
z_3^E (kg)	0	0	0
p^{DG} (kW)	5	5	5
\overline{p}^{DG} (kW)	20	10	15
MUT^{DG} (min)	10	10	10
MDT^{DG} (min)	10	10	10
C^{STU_DG} (¢)	100	100	100
C^{SHD_DG} (¢)	100	100	100

TABLE II

VALUE OF THE PARAMETERS OF THE SYSTEM AND PROBLEM.

n_t	288	$\overline{p}_{Type 1}^{PEV}$ (kW)	10	$SOC_{t_{Arr}}^{PEV}$ (%)	50
n_τ	12	$\overline{p}_{Type 2}^{PEV}$ (kW)	15	$\Delta t_{Dep-Arr}$	9-10, 16-17
φ	0.5	$Cap_{Type 1}^{PEV}$ (kWh)	50	Pr^{PEV} (¢)	200,000
β^E (¢/kg)	1	$Cap_{Type 2}^{PEV}$ (kWh)	75	ξ^{PEV} (Ah)	10,000
\overline{p}_2^{PV} (kW)	10	DOD^{PEV} (%)	20		
\overline{p}_3^{PV} (kW)	10	$SOC_{t_{Dep}}^{PEV}$ (%)	100		

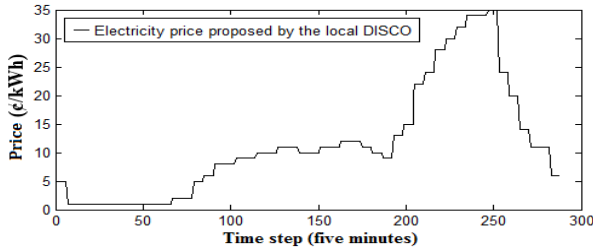


Fig. 6. The electricity price proposed by the local DISCO.

TABLE III

THE OPERATION COST OF EVERY SH AND THE SYSTEM (\$/DAY).

Energy scheduling	SH 1	SH 2	SH 3	SH 4	SH 5	Total
Without energy scheduling	10.21	11.47	14.54	13.38	16.38	66.01
Non-cooperative	-3.54	11.47	13.76	13.38	8.52	43.59
Cooperative distributed	-4.66	9.52	10.20	10.55	5.21	30.82

As can be seen in Fig. 7, the DG of SH 1 is shut down in 7th time step and the needed electricity is purchased from the local DISCO between the 7th-78th time steps of the operation period. For the rest of the operation period, SH 1 starts up its DG, supplies its demand, and exports its extra power to the connected SHs and the local DISCO, as can be seen in Figs. 7 and 8. As can be seen in Fig. 10, SH 2 purchases its needed power from the local DISCO just between 7th-78th time steps and in the other time steps, it purchases most of the demanded electricity from the connected SHs. In addition, SH 2 never sales electrical energy to the connected SHs or the local

DISCO. As can be seen in Fig. 11, the DG is turned off and on several times over the operation period, since this DG is the most expensive and pollutant DG. As can be seen in Fig. 13, the battery of PEV is charged between 121th-132th and 205th-216th time steps because the PEV has lost energy after it has been used by the driver. However, the battery of PEV does not have any charging and discharging pattern. As can be seen in Fig. 15, SH 5 starts up its DG in 103th time step and keeps it "on" until 282th time step; however, in some periods, sets the power of the DG at minimum power limit and avoids shutting it down. In addition, the battery of the PEV in SH 5 has the same charging patterns as SH 4.

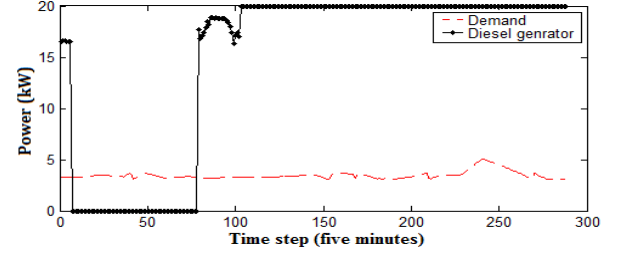


Fig. 7. The demand level and optimal power of energy sources in SH 1.

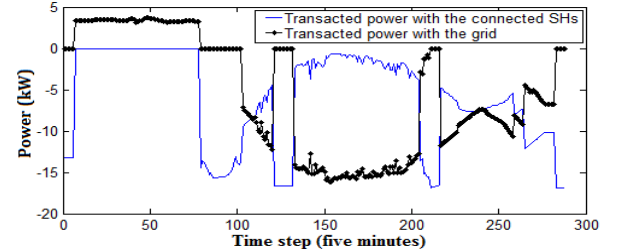


Fig. 8. The optimal transacted powers between SH 1 and the connected SHs and local DISCO.

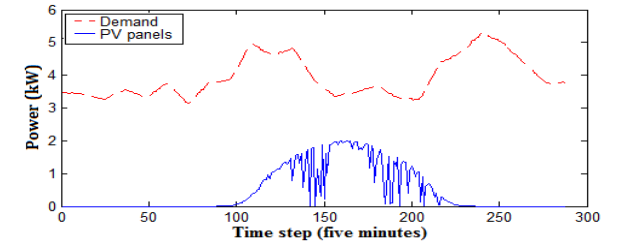


Fig. 9. The demand level and optimal power of energy sources in SH 2.

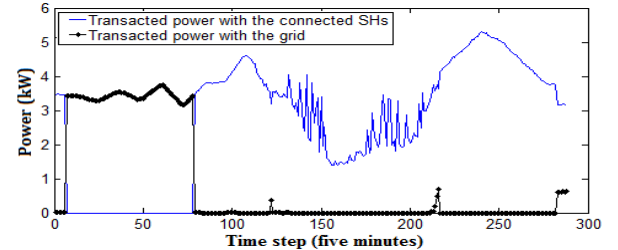


Fig. 10. The optimal transacted powers between SH 2 and the connected SHs and local DISCO.

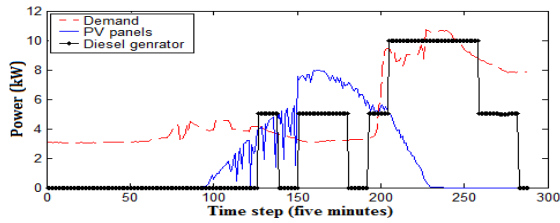


Fig. 11. The demand level and optimal power of energy sources in SH 3.

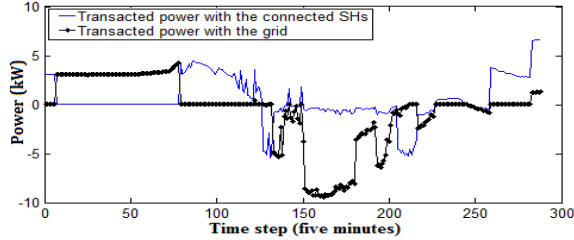


Fig. 12. The optimal transacted powers between SH 3 and the connected SHs and local DISCO.

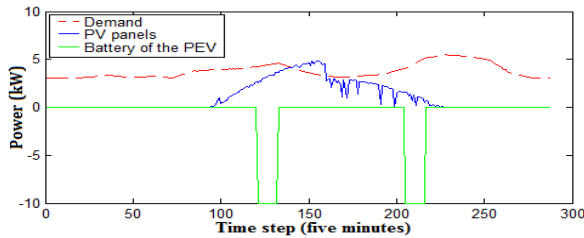


Fig. 13. The demand level and optimal power of energy sources in SH 4.

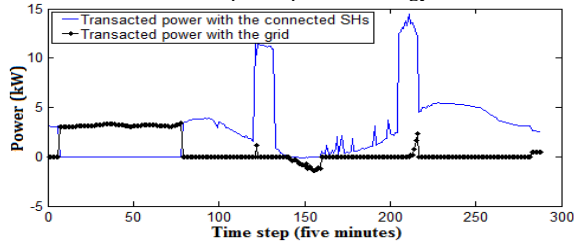


Fig. 14. The optimal transacted powers between SH 4 and the connected SHs and local DISCO.

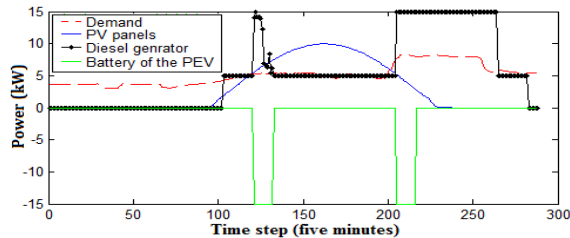


Fig. 15. The demand level and optimal power of energy sources in SH 5.

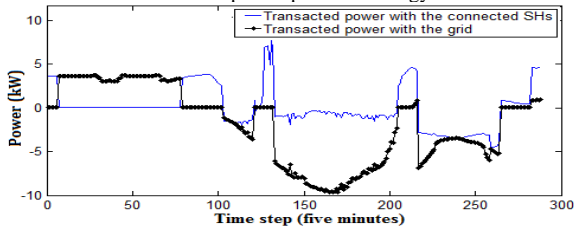


Fig. 16. The optimal transacted powers between SH 5 and the connected SHs and local DISCO.

V. CONCLUSION

In this study, the stochastic MPC as the adaptive and dynamic optimization technique was applied in the cooperative distributed energy scheduling problem of the set of SHs with different sources of energy to address the uncertainty and variability issues of the power of PV panels.

After simulating the problem, it was observed that cooperation of the SHs with one another in the distributed energy scheduling problem result in considerable cost saving. In fact, the reason for this achievement is related to the cooperation of the SHs for sharing their energy sources including DG, PV panels, and the battery of the PEV.

A suggestion for the future work, is applying a multi-time scale stochastic MPC with short and long time step durations to simultaneously have vast vision for the optimization time horizon and small scale resolution for the problem variables to improve the performance of each battery, since the batteries had limited performance because of short time scale of MPC.

Acknowledgements

This research was supported in part by U.S. NSF grants NSF-1404981, IIS-1354123, CNS-1254006, IBM Faculty Award 5501145 and Microsoft Research Faculty Fellowship 8300751.

REFERENCES

- [1] D. Pengwei, L. Ning. "Appliance commitment for household load scheduling," *IEEE Trans Smart Grid*, vol. 2, pp. 411-419, 2011.
- [2] A. Zipperer, P. A. Aloise-Young, S. Suryanarayanan, R. Roche, L. Earle, D. Christensen, P. Bauleo, and D. Zimmerle, "Electric energy management in the SH: Perspectives on enabling technologies and consumer behavior," *Proceedings of the IEEE*, vol. 101, no. 11, pp. 2397-2408, 2013.
- [3] U.S. Energy Information Administration, "Annual energy review 2011," Washington, DC, EIA-0384, Sep. 2012.
- [4] OECD/IEA, International Energy Agency, 2013. [Online]. Available: <http://www.iea.org/aboutus/faqs/energyefficiency>.
- [5] [Online]. Available: <http://www.homes.com/blog/2012/08/7-recent-advances-in-home-security-technology/>
- [6] U.S. Congress, H. R. 6, "Energy Independence and Security Act of 2007," *110th Congress, 1st Session*, Jan. 4, 2007. [Online]. Available: <http://www.gpo.gov/fdsys/pkg/BILLS-110hr6enr/pdf/BILLS-110hr6enr.pdf>.
- [7] L. Jiang, D. Y. Liu, and B. Yang, "Smart home research," in *Proc. 2004 Int. Conf. Mach. Learn. Cybern.*, vol. 2, pp. 659-663, 2004.
- [8] Federal energy regulatory commission, [Online]. Available: <http://www.ferc.gov/industries/electric/indus-act/section-1241.pdf>.
- [9] Y. Liu, S. Hu, H. Huang, R. Ranjan, A. Y. Zomaya, and Lizhe Wang, "Game-theoretic market-driven SH scheduling considering energy balancing," *IEEE System Journal*, DOI: 10.1109/JSYST.2015.2418032.
- [10] M. A. A. Pedrasa, T. D. Spooner, and I. F. MacGill, "Coordinated scheduling of residential distributed energy resources to optimize SH energy services," *IEEE Trans. Smart Grid*, vol.1, no.2, pp.134-143, 2010.
- [11] N. Gatsis and G. B. Giannakis, "Residential load control: Distributed scheduling and convergence with lost AMI messages," *IEEE Trans. Smart Grid*, vol. 2, no. 3, pp. 1-17, Feb. 2012.
- [12] T. Chang, M. Alizadeh, and A. Scaglione, "Real-time power balancing via decentralized coordinated home energy scheduling," *IEEE Trans. Smart Grid*, vol. 4, pp. 1490-1504, 2013.
- [13] M. Rahmani-andebili and H. Shen, "Energy scheduling for a smart home applying stochastic model predictive control," *The 25th International Conf. on Computer Communication and Networks (ICCCN)*, Waikoloa, Hawaii, USA, Aug. 1-4, 2016.
- [14] L. Chua and L. Yang, "Cellular neural networks," *IEEE international symposium on circuits and systems*, vol. 2, pp. 985-988, 1998.
- [15] M. Lisovich, D. Mulligan, and S. B. Wicker, "Inferring personal information from demand response systems," *IEEE Security and Privacy Magazine*, 2010.
- [16] J. B. Rawlings and D. Q. Mayne, "Model predictive control: Theory and design," Nob Hill Publishing, LLC, Madison, WI, 2009.
- [17] M. Rahmani-andebili, and G. K. Venayagamoorthy, Stochastic optimization for combined economic and emission dispatch with renewables, *IEEE Symposium Series on Computational Intelligence*, Cape Town, pp. 1252-1258, 2015.
- [18] Mitchell, Melanie (1996). An Introduction to Genetic Algorithms. Cambridge, MA: MIT Press. ISBN 9780585030944.
- [19] A. J. Wood and B. F. Wollenberg, Power Generation, Operation and Control, 2nd ed. New York: Wiley, 1996.